

CAS MCSCF/CAS MCQDPT2 Study of the Mechanism of Singlet Oxygen Addition to 1,3-Butadiene and Benzene

Maciej Bobrowski,^{†,‡} Adam Liwo,^{*,†} Stanisław Ołdziej,[†] Danuta Jeziorek,[§] and Tadeusz Ossowski[†]

Contribution from the Faculty of Chemistry, University of Gdańsk, Sobieskiego 18, 80-952 Gdańsk, Poland, Academic Computer Center in Gdańsk TASK, Technical University of Gdańsk, ul. Narutowicza 11/12, 80-952 Gdańsk, Poland, and Institute of Physics, Nicholas Copernicus University, ul. Grudziadzka 5, 87-100 Toruń, Poland

Received April 5, 2000

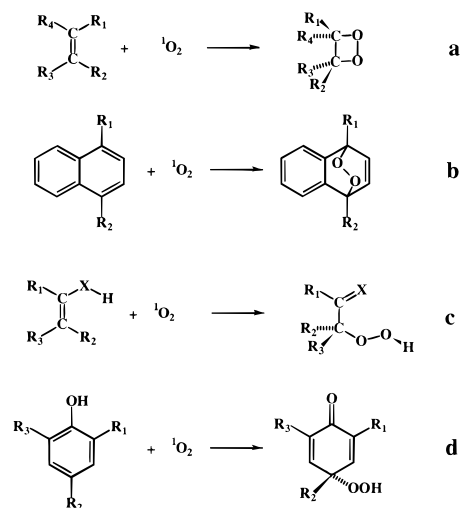
Abstract: The 1,4-cycloaddition reactions of the singlet ($^1\Delta_g$) oxygen with *s-cis*-1,3-butadiene and benzene, with the formation of 3,6-dihydro[1,2]dioxin and 2,3-dioxabicyclo[2.2.2]octa-5,7-diene, respectively, were studied by means of the CAS MCSCF/CAS MCQDPT2 ab initio method with the 6-31G* basis set. In the case of butadiene the reaction was found to be exoenergetic and the product was found to have C_2 symmetry, with the peroxide moiety in the gauche configuration. In the case of benzene the reaction was found to be endoenergetic and the bicyclic product formed was found to have C_{2v} symmetry, with the peroxide moiety in the syn configuration. Three possible reaction routes were studied: (i) concerted cycloaddition, (ii) stepwise cheletropic cycloaddition with the formation of zwitterionic 2,5-dihydrofuran I-oxide as an intermediate, and (iii) stepwise cycloaddition with the formation of a linear intermediate. In the case of butadiene routes (i) and (ii) were excluded, because only second-order saddle points were found on the corresponding reaction pathways. The linear intermediate (I_1) found in route (iii) has a biradical character, and its energy relative to that of the separate reactants is 4.1 kcal/mol. The dominant activation barrier corresponds to the transition structure T_1 leading to I_1 and amounts to 9.9 kcal/mol. The rearrangement of I_1 to the product (P) involves only a minor activation barrier of 7.5 kcal/mol (relative to I_1). In the case of benzene the reaction occurs in a concerted manner with a single transition structure having C_{2v} symmetry; the activation barrier is 25.3 kcal/mol. This difference in binding mechanism can be explained in terms of the configuration of the peroxide moiety in the adduct.

Introduction

Singlet ($^1\Delta_g$) oxygen addition to unsaturated and aromatic compounds, which involves the formation of organic peroxides and hydroperoxides, plays an important role in chemical and biochemical processes.^{1–3} Singlet oxygen addition to lipids and other unsaturated components of the living cells can directly initiate the chain of radical reactions leading to peroxidation,^{1,4} while oxygen addition to xenobiotics can result in the generation of superoxide anion radicals and other active oxygen species of high cytotoxicity.

The four principal types of oxygen addition reactions are (i) $[\pi 2 + \pi 2]$ 1,2-cycloaddition to an isolated double bond, resulting in the formation of 1,2-peroxides (Scheme 1a); (ii) 1,4-cycloaddition to a system containing at least two conjugated double bonds, resulting in the formation of the so-called 1,4-peroxides (Scheme 1b); (iii) 1,3-addition to a double bond connected to a hydrogen-bearing group, resulting in the formation of allylic hydroperoxides (Scheme 1c); and (iv) 1,4-addition to phenols and naphthols with the formation of hydroperoxide

Scheme 1. Examples of the Addition of Oxygen to Unsaturated and Aromatic Compounds



^a 1,2-Addition to olefins to form 1,2-dioxetane-type products. ^b 1,4-Addition to naphthalene derivatives to form 1,4-endoperoxides. ^c 1,3-Addition to olefin derivatives; X denotes CR₂, NR, or O. ^d Addition to phenol derivatives containing bulky groups in positions 2 and 4 of the ring to form hydroperoxide ketones.

ketones (Scheme 1d). The formation of 1,4-peroxides and hydroperoxide ketones from naphthalene and anthracene derivatives or phenols and naphthols, respectively, occurs readily when oxygen is passed through UV-irradiated, cooled nonaqueous

* To whom correspondence should be addressed.

[†] University of Gdańsk.

[‡] Technical University of Gdańsk.

[§] Nicholas Copernicus University.

(1) Halliwell, B.; Gutteridge, J. M. C. *Free radicals in biology and medicine*; Clarendon Press: Oxford, 1985.

(2) Kearns, D. R. *Chem. Rev.* **1971**, *71*, 395–427.

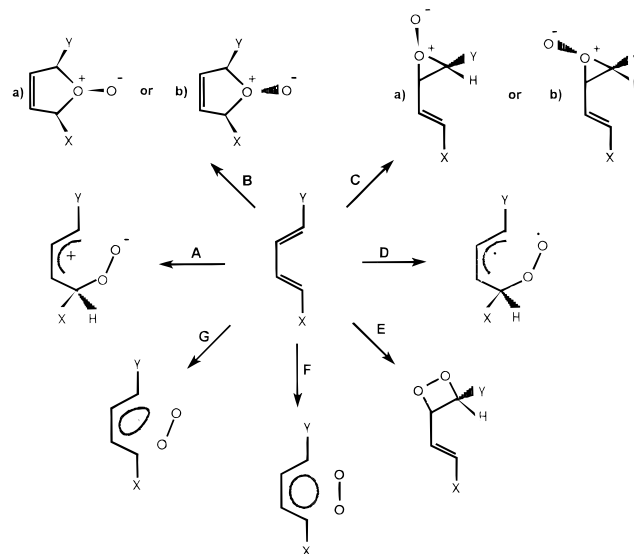
(3) Lissi, E. A.; Encinas, M.; Lemp, E.; Rubio, M. A. *Chem. Rev.* **1993**, *93*, 699–723.

(4) Pryor, W. A., Ed. *Free radicals in biology*; Academic Press: New York, 1982; Vol. V.

solutions of naphthalene or anthracene derivatives^{5–7} or phenols or naphthols,^{7,8} respectively.

There have been numerous experimental^{2,9–11} and theoretical^{12–20} studies on 1,2-cycloaddition. On the basis of the results of their MCSCF study of oxygen addition to ethene¹⁷ and, very recently, ethene derivatives and butadiene,²⁰ Tonachini and co-workers concluded that the reaction occurs through a biradicaloid intermediate, in which one oxygen atom is attached to one end of the C=C bond. A linear intermediate of the same type was found in our MCSCF study of singlet oxygen addition to ethenol.¹⁹ We found that in this case either the intermediate can undergo ring closure to form the 1,2-peroxide or a proton transfer to the peroxy moiety can occur to form the hydroperoxide, the latter product having considerably lower energy. Only one MINDO/3-CI¹² and one ab initio UMP2 study²¹ of oxygen addition to butadiene and one semiempirical and DFT study of oxygen addition to benzene²² have been reported, and no study has been carried out at the MCSCF level. The above-mentioned study by Tonachini and co-workers²⁰ included butadiene but considered only the [$\pi 2 + \pi 2$] cycloaddition and not the [$\pi 4 + \pi 2$] cycloaddition of oxygen to butadiene. Therefore, we devoted our present study to the investigation of the mechanism of singlet oxygen 1,4-addition to *cis*-1,3-butadiene to form 3,6-dihydro[1,2]dioxin and to benzene to form 2,3-dioxabicyclo[2.2.2]octa-5,7-diene using the CAS MCSCF/CAS MCQDPT2 ab initio method. These reactions can be considered model reactions of 1,4-oxygen addition to conjugated and aromatic systems, respectively. The choice of simple models, which however possess all the essential features of more complicated systems, enables one to apply a high level of theory, which is necessary to achieve a correct qualitative description of the energy surfaces of the reactions under study. Nevertheless, it

Scheme 2. Schematic Representation of Possible Mechanisms of Oxygen Binding to Conjugated Double Bonds^a



^a See text for description.

should be noted that the simple systems chosen correspond exactly to the reactions observed experimentally. Addition of oxygen to butadiene to form 3,6-dihydro[1,2]dioxin was carried out by Kondo et al. with 20% yield.²³ Although oxygen addition to benzene itself has not been observed experimentally, because of the high ionization potential of this compound, oxygen addition to pentamethyl- and hexamethylbenzene, which have considerably lower ionization potentials, occurs readily with initial formation of the corresponding endoperoxides, which have been detected experimentally.²⁴ These two compounds have the same π -electronic structure as benzene.

Scheme 2 summarizes intermediates or transition structures (and thereby the respective reaction mechanisms) in oxygen [$\pi 4 + \pi 2$] cycloaddition to conjugated double bonds proposed in the literature.²⁵ Mechanisms A and D involve zwitterionic or biradical linear intermediates, respectively; they should be nonstereospecific, which was, indeed, observed in the reaction of singlet oxygen with (*E,Z*)-2,4-hexadiene.²⁶ Mechanisms F and G are concerted mechanisms, involving symmetric or nonsymmetric transition structures, respectively; they are supported by the stereospecificity of [$\pi 4 + \pi 2$] oxygen cycloadditions to condensed or sterically hindered dienes.^{27,28} Moreover, a concerted symmetric cycloaddition mechanism was found by Houk and co-workers in their ab initio UMP2 study²¹ of oxygen [$\pi 4 + \pi 2$] addition to *cis*-1,3-butadiene. Mechanism C involves peroxiranes and was proposed by Dewar and Thiel,¹² on the basis of the results of their MINDO/3-CI calculations. However, this mechanism can be excluded on the basis of the results of the recent study of Tonachini and co-workers.²⁰ Mechanism E involves dioxetane intermediates; however, vinyl dioxetanes isolated by Kearns²⁹ and Clennan³⁰ decomposed without rear-

- (5) Gérard, M.; Dufraisse, C. *C. R. Acad. Sci.* **1935**, *201*, 428–430.
 (6) Brown, C. J.; Ehrenberg, M. *Acta Crystallogr.* **1984**, *C40*, 1059–1060.
 (7) Saito, I.; Kato, S.; Matsuura, T. *J. Am. Chem. Soc.* **1983**, *105*, 3200–3206.
 (8) (a) Saito, I.; Kato, S.; Matsuura, T. *Tetrahedron Lett.* **1970**, 239–242. (b) Kharasch, M. S.; Joshi, B. S. *J. Org. Chem.* **1957**, *22*, 1439–1443. (c) Thomas, M. J.; Foote, C. S. *Photochem. Photobiol.* **1978**, *27*, 683–693. (d) Clough, R. L.; Yee, B. G.; Foote, C. S. *J. Am. Chem. Soc.* **1979**, *101*, 683–686. (e) Jensen, F.; Foote, C. S. *Photochem. Photobiol.* **1987**, *46*, 325–330. (f) Dowd, P.; Ham, S. W.; Geib, S. J. *J. Am. Chem. Soc.* **1991**, *113*, 7734–7743.
 (9) Bartlett, P. D.; Schaap, A. P. *J. Am. Chem. Soc.* **1970**, *92*, 3223–3225.
 (10) (a) Frimer, A. A. *Chem. Rev.* **1979**, *79*, 359–472 and references therein. (b) Frimer, A. A.; Stephenson, L. M. In *Singlet O₂*; Frimer, A. A., Ed.; CRC Press Inc.: Boca Raton, FL, 1985; Vol. II, Part 1, Chapter 3, pp 67–91.
 (11) Jefford, C. W. *Chem. Soc. Rev.* **1993**, 59–66 and references therein.
 (12) Dewar, M. J. S.; Thiel, W. *J. Am. Chem. Soc.* **1975**, *97*, 3978–3986.
 (13) Harding, L. B.; Goddard, W. A., III. *J. Am. Chem. Soc.* **1980**, *102*, 439–449.
 (14) Yamaguchi, K.; Yabushita, S.; Fueno, T.; Houk, K. N. *J. Am. Chem. Soc.* **1981**, *103*, 5043–5046.
 (15) Hotokka, M.; Roos, B.; Siegbahn, P. *J. Am. Chem. Soc.* **1983**, *105*, 5263–5269.
 (16) Bernardi, F.; Bottoni, A.; Olivucci, M.; Robb, M.; Schlegel, H. B.; Tonachini, G. *J. Am. Chem. Soc.* **1988**, *110*, 5993–5995.
 (17) Tonachini, G.; Schlegel, H. B.; Bernardi, F.; Robb, M. A. *J. Am. Chem. Soc.* **1990**, *112*, 483–491.
 (18) Yoshioka, Y.; Yamada, S.; Kawakami, T.; Nishino, M.; Yamaguchi, K.; Saito, I. *Bull. Chem. Soc. Jpn.* **1996**, *69*, 2683–2699.
 (19) Liwo, A.; Dyl, D.; Jeziorek, D.; Nowacka, M.; Ossowski, T.; Woźnicki, W. *J. Comput. Chem.* **1997**, *18*, 1668–1681.
 (20) Maranzana, A.; Ghigo, G.; Tonachini, G. *J. Am. Chem. Soc.* **2000**, *122*, 1414–1423.
 (21) McCarrick, M. A.; Wu, Y. D.; Houk, K. N. *J. Org. Chem.* **1993**, *58*, 3330–3343.
 (22) Cheikh, F.; Boucekkine, A.; Cartier, A. *J. Mol. Struct. THEOCHEM* **1997**, *397*, 13–20.

- (23) Kondo, T.; Matsumoto, M.; Mitsuoshi, T. *Tetrahedron Lett.* **1978**, *40*, 3819–3822.
 (24) Van den Heuvel, C. J. M.; Hofland, A.; Steinberg, H.; de Boer, T. *J. Recl. Trav. Chim. Pays-Bas* **1980**, *99*, 275–278.
 (25) Clennan, E. L. *Tetrahedron* **1991**, *47*, 1343–1382.
 (26) Gollnick, K.; Griesbeck, A. *Tetrahedron Lett.* **1983**, *24*, 3303–3306.
 (27) Gollnick, K.; Schenck, G. O. In *1,4-Cycloaddition Reactions*; Hamer, J., Ed.; Academic Press: Orlando, FL, 1967; pp 255–344.
 (28) Rigaudy, J.; Capdevielle, P.; Cambrissin, S.; Maumy, M. *Tetrahedron Lett.* **1974**, 2757–2760.
 (29) Hasty, N. M.; Kearns, D. R. *J. Am. Chem. Soc.* **1973**, *95*, 3380–3381.

angement, rendering this mechanism unlikely. Mechanism B involves cheletropic addition of oxygen, with the formation of zwitterionic substituted 2,5-dihydrofuran 1-oxide intermediates. Although there is no direct experimental evidence to support this mechanism, it could be considered possible, because it occurs in some other cycloaddition reactions.²⁵

Because the experimental data do not provide full evidence as to whether concerted mechanisms (F and G) or those involving linear intermediates (A and D) take place, we investigated the corresponding pathways. We also investigated the cheletropic mechanism B, which was not considered previously in theoretical studies.

Methods

Calculations were carried out at the CAS MCSCF level, with the 6-31G* basis set. In our previous study¹⁹ we found that introducing polarization functions is necessary to achieve correct geometry of the O—O moiety. As in our earlier study, we used the (10,8) active space (8 orbitals with 10 electrons) in most of the calculations. For isolated reactants, this active space corresponds to σ_o , $\pi_{\pm 1}$, $\pi_{\pm 1}^*$, and σ_o^* orbitals of the oxygen molecule and the HOMO—LUMO pair of the organic compound molecule. Additional calculations for butadiene, and those calculations for benzene, aimed at estimating the energies of the species relative to those of the reactants, were performed in an extended (12,10) active space obtained by adding the next bonding—antibonding π_2 — π_2^* orbital pair of the organic donor. This extension was necessary in the case of benzene, because of the double degeneracy of the HOMO and LUMO orbitals in the isolated benzene molecule. Considering only one HOMO—LUMO pair could therefore introduce a bias to the energy of benzene. It should be noted that because of symmetry breaking following oxygen interaction with benzene, all species on the benzene—oxygen reaction path (except the isolated benzene molecule) have nondegenerate energy levels; therefore, even the (10,8) active space is appropriate. For optimized geometries dynamic correlation was estimated by carrying out single-point MCQDPT2 calculations.³¹ The basis set superposition error (BSSE) was estimated by the method of Chalasinski et al.,³² as in our previous work.¹⁹

The six-fold symmetry of the benzene ring and the C_s symmetry of *s-cis* butadiene were kept during optimization of the structures of the reactants.

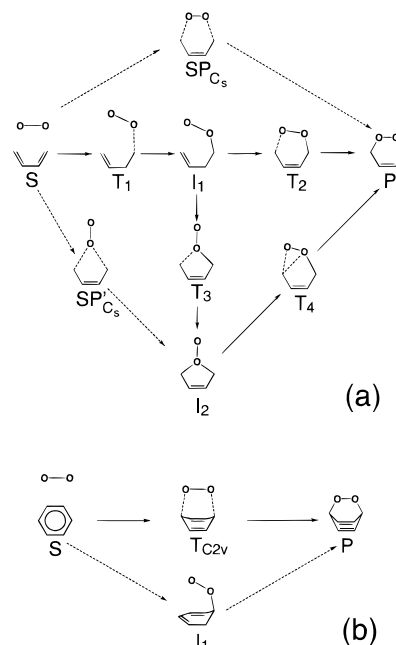
Transition structures were located by calculating energy profiles of the reacting systems in the internal coordinate most closely approximating the appropriate reaction coordinate, with optimization of all remaining degrees of freedom. The geometry corresponding to the maximum in the energy curve was taken as an initial approximation to that of the transition structure, and then the gradient norm was minimized to complete the search of the transition structure. The Hessian matrix and subsequently the normal modes were calculated for all stationary points. The Hessian matrix was evaluated numerically. Finally, for transition structures, intrinsic reaction path (IRC) calculations were carried out to make sure that the transition structures are located between the correct energy minima.

All calculations were carried out with the use of the program GAMESS.³³

Results and Discussion

Oxygen Cycloaddition to *s-cis* 1,3-Butadiene. The reaction routes connecting the stationary points found in the reaction paths studied are presented in Scheme 3a. The calculated

Scheme 3. Outline of the Reaction Routes Studied Here Corresponding to Oxygen Addition to *cis*-1,3-Butadiene (a) and Benzene (b)^a



^a The broken lines in part (a) indicate that the corresponding stationary points are only second-order saddle points. The broken-line arrows in part (b) indicate that no path connecting I_1 with $T_{C_{2v}}$ or P was found.

structures of intermediates and transition structures are shown in Figure 1 (with 3,6-dihydro[1,2]dioxin as the final product), and the energies are summarized in Table 1. The product has C_2 symmetry, with the rotation axis passing through the centers of the middle C—C bond and the O—O bond (Figure 1d). This result is consistent with the crystal structures of monocyclic peroxides formed from 1,3-dienes³⁴ (as found in the Cambridge Structural Database³⁵). According to the results of the calculations, the reaction is significantly exoenergetic (Table 1). The reaction involves the formation of a linear intermediate (I_1), in which the oxygen molecule is attached to one of the terminal carbon atoms (Figure 1b). Inspection of the configuration state functions (CSFs) and natural orbital occupancies (Tables 2 and 3) reveals that I_1 and the transition structure T_1 from the reactants to I_1 have an open-shell character, with the two outermost orbitals b_1 and b_2 approximately half-filled (see Scheme 4 for pictorial representation of composite orbitals). Their effective electronic configuration can be approximated by $\sigma_{2p_x}(O_2)^2\pi_{2p_y}-(O_2)^2\pi_{2p_z}(O_2)^2\sigma_{2p_x}(CO)^2b_1^1b_2^1$ (see the legend to Table 3 and Scheme 4 for the character of orbitals of T_1 and I_1). As in the case of oxygen addition to ethenol,¹⁹ the b_1 and b_2 orbitals are linear combinations of the $\pi_{2p_y}^*$ orbital of the oxygen moiety and the $2p_z$ orbital of the middle carbon atom closest to the C—O bond. After the rotations of the —CH₂—O—O group about the CH—CH₂ and the CH₂—O bonds, the $2p_z$ orbital of the outermost oxygen atom begins to overlap with the $2p_z$ orbital of the outermost carbon atom in the T_2 transition structure and, finally, in the formation of the second C—O bond in P.

(30) Clennan, E. L.; L'Esperance, R. P. *J. Am. Chem. Soc.* **1985**, *107*, 5178–5182.

(31) (a) Nakano, H. *J. Chem. Phys.* **1993**, *99*, 7983–7992. (b) Nakano, H. *Chem. Phys. Lett.* **1993**, *207*, 372–378.

(32) Chalasinski, G.; Kendall, R. A.; Simons, J. *J. Chem. Phys.* **1987**, *87*, 2965–2975.

(33) Schmidt, M. W.; Baldridge, K. K.; Boatz, J. A.; Elbert, S. T.; Gordon, M. S.; Jensen, J. J.; Koseki, S.; Matsunaga, N.; Nguyen, K. A.; Su, S.; Windus, T. L.; Dupuis, M.; Montgomery, J. A. *J. Comput. Chem.* **1993**, *14*, 1347–1363.

(34) (a) Perales, A.; Martinez-Ripoll, M.; Fayos, J.; Savona, G.; Bruno, M.; Rodriguez, B. *J. Org. Chem.* **1983**, *48*, 5318–5371. (b) Zadok, E.; Rubinaut, S.; Frolow, F.; Mazur, Y. *J. Org. Chem.* **1985**, *50*, 2647–2649. (c) Sterns, M. *J. Cryst. Mol. Struct.* **1973**, *1*, 373–381. (d) Adembri, G.; Celli, A. M.; Donati, D.; Scotton, M.; Segal, A. *Acta Crystallogr., Sect. C* **1987**, *43*, 69–71.

(35) Allen, F. H.; Kennard, O.; Taylor, R. *Acc. Chem. Res.* **1983**, *16*, 146–184.

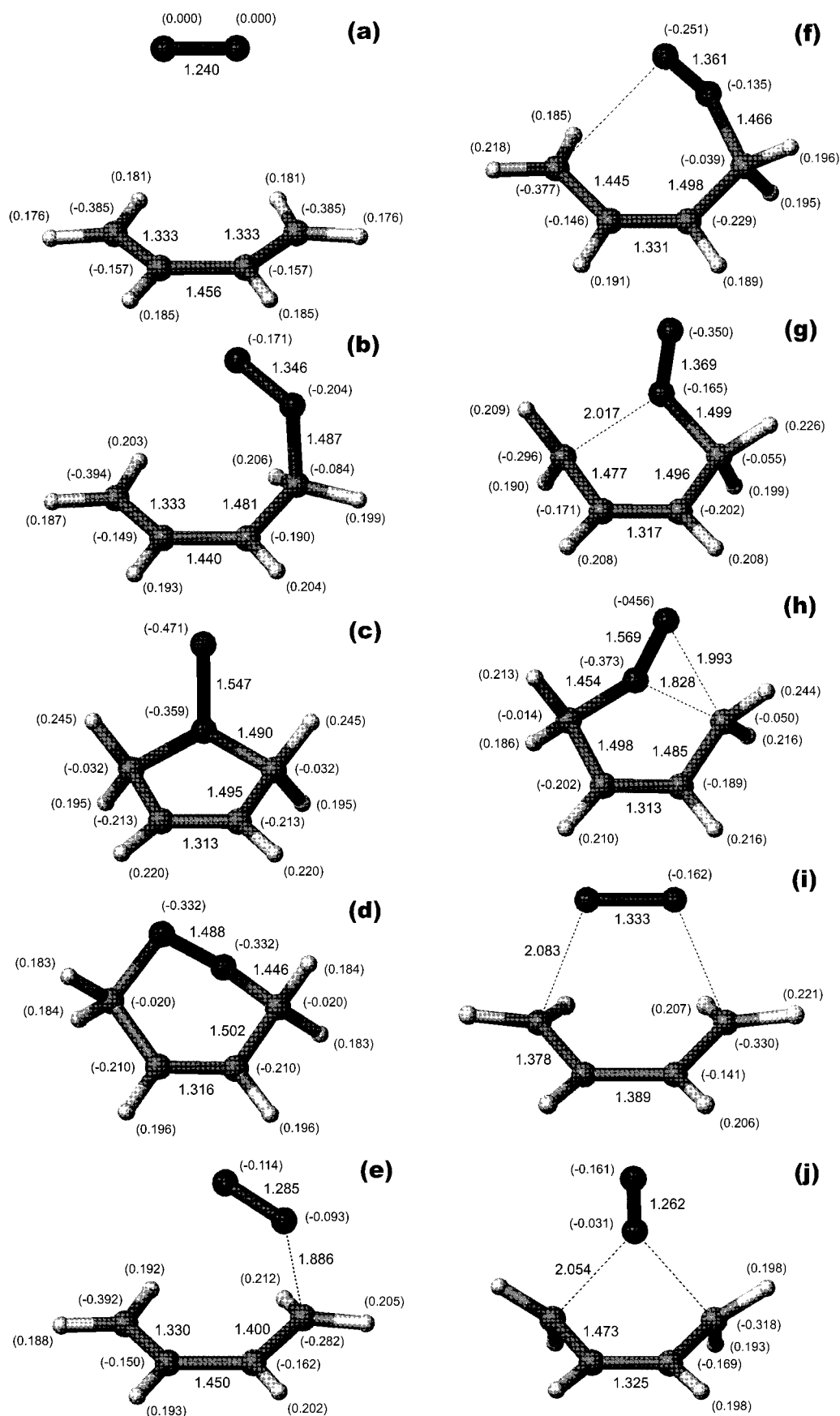


Figure 1. Stationary points on the 1,3-butadiene-singlet oxygen energy surface: (a) the reactants (S), (b) the linear intermediate (I_1), (c) the “chelatic” intermediate (I_2), (d) the product (P), (e) the transition structure from S to I_1 (T_1), (f) the transition structure from I_1 to P (T_2), (g) the transition structure from I_1 to I_2 (T_3), (h) the transition structure from I_2 to P (T_4), (i) the *supra-supra* second-order saddle point from S to P (SP_C), and (j) the second-order saddle point from S to I_2 (SP'_C). The lengths of selected bonds, selected interatomic distances in transition structures, and Mulliken population charges (in parentheses) are shown. The drawings were generated using MOLMOL.⁴⁰

Table 1. Relative Energies (with Respect to the Separated Reactants; kcal/mol) of the Stationary Points in Oxygen 1,4-Addition to 1,3-Butadiene

species		ΔE_{MCSCF}	$\Delta E_{\text{MCSCF/BSSE}}$	$\Delta E_{\text{MCQDPT2}}$	$\Delta E_{\text{MCQDPT2/BSSE}}$
second-order saddle point	SP_{C_s}	22.20	23.37	7.74	10.90
transition structure	T_1	16.23	17.92	4.71	9.91
diracal intermediate	I_1	4.60	6.92	-3.63	4.09
transition structure	T_2	10.26	21.02	3.10	11.54
second-order saddle point	SP'_{C_s}	39.76	41.52	22.04	28.20
transition structure	T_3	23.60	26.07	12.35	22.90
zwitterionic intermediate	I_2	-4.35	-1.49	-2.80	11.11
transition structure	T_4	32.15	35.06	29.70	41.56
cyclic product	P	-44.84	-41.70	-52.05	-38.01

Table 2. Dominant Configuration State Functions^a of All Stationary States in Oxygen 1,4-Addition to 1,3-Butadiene

structure		CSF								coeff.
diradical intermediate	I_1	2	2	2	2	2	0	0	0	0.8078
zwitterionic intermediate	I_2	2	2	2	2	2	0	0	0	-0.5363
cyclic product	P	2	0	2	2	2	2	0	0	0.9726
transition structure	T_1	2	0	2	2	2	0	0	2	-0.1318
transition structure	T_2	2	2	2	2	2	0	0	0	0.9660
transition structure	T_3	2	2	2	2	2	0	0	0	-0.1790
transition structure	T_4	2	2	2	2	2	0	0	0	0.8831
second-order saddle point	SP_{C_s}	2	2	2	2	2	0	0	0	-0.3290
second-order saddle point	SP'_{C_s}	2	2	2	2	2	0	0	0	-0.1012
second-order saddle point	SP'_{C_s}	2	2	2	2	2	0	0	0	0.1004
second-order saddle point	SP'_{C_s}	2	2	2	2	2	0	0	0	0.7949
second-order saddle point	SP'_{C_s}	2	2	2	2	2	0	0	0	-0.5580
second-order saddle point	SP'_{C_s}	2	0	2	2	2	0	0	2	-0.1057
second-order saddle point	SP'_{C_s}	2	1	2	1	1	1	0	1	-0.1012
second-order saddle point	SP'_{C_s}	2	2	2	2	2	0	0	0	0.9108
second-order saddle point	SP'_{C_s}	2	2	2	2	2	0	0	0	-0.3245
second-order saddle point	SP'_{C_s}	2	1	2	1	2	1	0	1	-0.1127
second-order saddle point	SP'_{C_s}	2	0	2	2	2	0	0	2	-0.1076
second-order saddle point	SP'_{C_s}	2	2	2	2	2	0	0	0	0.9587
second-order saddle point	SP'_{C_s}	2	0	2	2	2	0	2	0	-0.1563
second-order saddle point	SP'_{C_s}	2	2	2	2	2	0	0	0	0.9303
second-order saddle point	SP'_{C_s}	0	2	2	2	2	2	0	0	-0.1744
second-order saddle point	SP'_{C_s}	2	2	2	0	2	0	2	0	-0.1290
second-order saddle point	SP'_{C_s}	1	2	2	1	2	1	2	0	-0.1161
second-order saddle point	SP'_{C_s}	2	0	2	2	2	0	0	2	-0.1112
second-order saddle point	SP'_{C_s}	1	1	2	2	2	1	0	1	0.1094
second-order saddle point	SP'_{C_s}	1	2	2	1	2	1	1	0	0.1000
second-order saddle point	SP'_{C_s}	2	2	2	2	2	0	0	0	0.8449
second-order saddle point	SP'_{C_s}	2	2	2	1	1	1	1	0	-0.2858
second-order saddle point	SP'_{C_s}	2	2	2	2	0	0	2	0	-0.2114
second-order saddle point	SP'_{C_s}	2	2	2	0	2	2	0	0	-0.1911
second-order saddle point	SP'_{C_s}	2	2	2	1	1	1	0	1	0.1319
second-order saddle point	SP'_{C_s}	2	2	2	0	0	2	2	0	0.1275
second-order saddle point	SP'_{C_s}	2	2	2	2	0	2	0	0	-0.1257
second-order saddle point	SP'_{C_s}	2	2	2	0	2	0	2	0	-0.1024

^a The CSFs with coefficients greater than 0.1 in absolute value. See Table 3 for the order and description of orbitals.

There is no concerted pathway from the reactants to the product (P), because the corresponding “would-be” transition structure, SP_{C_s} , is a second-order saddle point. This stationary point has a largely closed-shell character, and its effective configuration is $\sigma_{2p_x}(\text{O}_2)^2\pi_{2p_y}(\text{O}_2)^2\pi_{2p_z}(\text{O}_2)^2\sigma_4^2\pi_{2p_y}^*(\text{O}_2)^2$ (Table 3). It should be noted that only one bonding orbital that pertains to the two C–O bonds being formed (σ_4 ; Scheme 4) becomes doubly filled. One of its electrons comes from the HOMO orbital of butadiene and another one from the $\pi_{2p_x}^*$ orbital of oxygen (the one most aligned with the C–O bonds). The remaining electron of the HOMO orbital of butadiene is transferred to the $\pi_{2p_y}^*$ orbital of oxygen (the one perpendicular to the C–O–O–C plane), which becomes doubly filled. This formally results in the transfer of a unit electron charge from butadiene to oxygen, which is reflected in increased negative charges of the oxygen atoms, compared with the charges of T_1 (Figure 1). Breaking the symmetry of the SP_{C_s} second-order saddle point changed the two C···O distances, until the transition structure

T_1 was reached. Oxygen addition to butadiene cannot, therefore, be considered a “classical” Diels–Alder [$\pi_4 + \pi_2$] cycloaddition. This result is different from that obtained by Houk and co-workers²¹ using the ab initio UMP2 method with the 6-31G* basis set; these authors found a concerted mechanism, as in the case of ethene addition to butadiene. (The concerted mechanism of the latter reaction has been proved by MCSCF ab initio³⁶ and DFT³⁷ calculations.) A stepwise mechanism of oxygen addition to butadiene was found in an earlier MINDO/3-CI study by Dewar and Thiel,¹² but that mechanism involved a closed-shell peroxirane intermediate and not a biradical linear one.

Although SP_{C_s} has a largely closed-shell character (Tables 2 and 3), calculations at a single-determinant reference level predicts only one normal mode with an imaginary frequency.²¹ It could therefore be suspected that using insufficient active space could lead to incorrect characteristics of SP_{C_s} . To check this, we extended the active space to (12,10) to include the second $\pi_2-\pi_2^*$ orbital pair of butadiene. After geometry optimization, SP_{C_s} remained a second-order saddle point, and the occupancies of additional pairs of orbitals (which, however, change their character on oxygen binding) were very close to 2 and 0, respectively. Because the completeness of the active space should be even more critical for definitely open-shell species, we also performed an additional geometry optimization of the true transition state, T_1 , with the (12,10) space. Again, the occupancies of the additional orbitals introduced to the active space remained close to 2 and 0, respectively, and T_1 remained a first-order saddle point. Therefore, using the (10,8) active space seems to be sufficient to study the mechanism of oxygen addition to butadiene.

It should be noted that, in contrast to the case for oxygen addition to ethene,^{17,20} the difference between the energies of T_1 and SP_{C_s} is only 1 kcal/mol (at the MCQDPT2/BSSE level; Table 1). Moreover, in the case of oxygen addition to ethene, the symmetric saddle point is a third-order saddle point.¹⁷ This is because the symmetric binding mode is forbidden in the case of oxygen addition to ethene, since there is no phase continuity of the overlapping HOMO orbital of ethene and the $\pi_{2p_x}^*$ orbital of O_2 , which are the first viable candidates to initiate bond formation. There is, therefore, a strong force, which leads to breaking the C_s symmetry of the transition structure and forming initially only one C–O bond. Conversely, the phases of the overlapping parts of the HOMO orbital of butadiene and the $\pi_{2p_y}^*$ orbital of oxygen are consistent, and overlap can develop to form the σ_4 molecular orbital. The presence of the second imaginary frequency of SP_{C_s} , which corresponds to rotating the peroxide moiety with respect to butadiene and altering the two C···O distances (Figure 2), can be explained by the fact that the symmetric binding mode would result only in the product with the C_s symmetry, which is a saddle point in the conformational transition between two equivalent conformations of the six-membered ring with the C_2 symmetry. Therefore, the oxygen-binding mechanism involves two stages. This also is confirmed by the fact that oxygen addition to linear dienes can occur nonstereospecifically.²⁵ The experimentally measured rate constants of oxygen binding to acyclic 1,3-dienes only weakly depend on solvent polarity,³ which suggests the biradical mechanism with little charge transfer, as opposed to the mechanism involving the symmetric SP_{C_s} second-order saddle point, in which charge transfer to oxygen is more pronounced (Figure 1i).

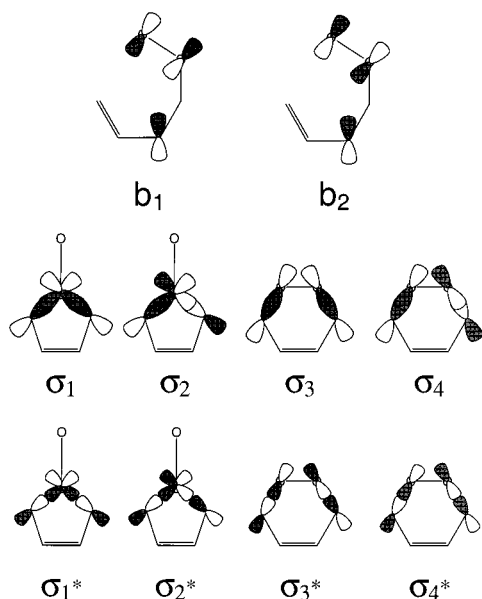
(36) Li, Y.; Houk, K. N. *J. Am. Chem. Soc.* **1993**, *115*, 7478–7485.

(37) Goldstein, E.; Benno, B.; Houk, K. N. *J. Am. Chem. Soc.* **1996**, *118*, 6036–6043.

Table 3. Character^a and Occupation Numbers of the MCSCF Natural Orbitals of All Stationary Structures in Oxygen 1,4-Addition to 1,3-Butadiene

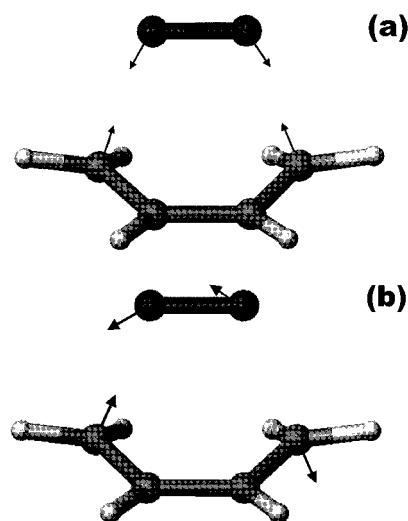
I ₁		I ₂		P		T ₁		T ₂	
$\sigma_{2s}(\text{O}_2)$	1.97	$\sigma_{2s}(\text{O}_2)$	2.00	$\sigma_{2s}(\text{O}_2)$	2.00	$\sigma_{2s}(\text{O}_2)$	1.99	$\sigma_{2s}(\text{O}_2)$	1.97
$\sigma_{2p_x}(\text{O}_2)$	1.94	$\sigma_{2p_x}(\text{O}_2)$	1.95	$\sigma_{2p_x}(\text{O}_2)$	1.92	$\sigma_{2p_x}(\text{O}_2)$	1.95	$\sigma_{2p_x}(\text{O}_2)$	1.94
$\pi_{2p_y}(\text{O}_2)$	2.00	$\pi_{2p_y}(\text{O}_2)$	1.97	$\pi_{2p_y}(\text{O}_2)$	2.00	$\pi_{2p_y}(\text{O}_2)$	1.95	$\pi_{2p_y}(\text{O}_2)$	2.00
$\sigma(\text{CO})$	1.97	σ_1	1.97	σ_3	1.97	$\sigma(\text{CO})$	1.92	σ_3	1.98
b ₁	1.39	σ_2	1.99	σ_4	1.97	b ₁	1.72	σ_4	1.35
b ₂	0.63	σ_2^*	0.03	σ_4^*	0.03	b ₂	0.32	σ_4^*	0.68
$\sigma^*(\text{CO})$	0.03	σ_1^*	0.05	σ_3^*	0.05	$\sigma^*(\text{CO})$	0.10	σ_3^*	0.03
$\sigma_{2p_x}^*(\text{O}_2)$	0.06	$\sigma_{2p_x}^*(\text{O}_2)$	0.02	$\sigma_{2p_x}^*(\text{O}_2)$	0.08	$\sigma_{2p_x}^*(\text{O}_2)$	0.05	$\sigma_{2p_x}^*(\text{O}_2)$	0.06
T ₃		T ₄		SP _{C_s}		SP' _{C_s}			
$\sigma_{2s}(\text{O}_2)$	1.97	$\sigma_{2s}(\text{O}_2)$	2.00	$\pi_{2p_y}(\text{O}_2)$	1.88	$\pi_{2p_y}(\text{O}_2)$	1.96		
$\sigma_{2p_x}(\text{O}_2)$	1.94	$\sigma_{2p_x}(\text{O}_2)$	1.92	$\sigma_{2p_x}(\text{O}_2)$	1.94	$\sigma_{2p_x}(\text{O}_2)$	1.95		
$\pi_{2p_y}(\text{O}_2)$	2.00	$\pi_{2p_y}(\text{O}_2)$	1.97	$\sigma_{2s}^*(\text{O}_2)$	1.99	$\pi_{2p_y}(\text{O}_2)$	1.97		
$\sigma(\text{CO})$	1.97	σ_1	1.99	σ_4	1.91	σ_1	1.76		
b ₁	1.77	σ_2	1.95	$\pi_g(\text{CC})$	1.99	σ_2	1.73		
b ₂	0.26	σ_2^*	0.03	σ_4^*	0.15	σ_1^*	0.29		
$\sigma^*(\text{CO})$	0.03	σ_1^*	0.09	σ_3^*	0.08	σ_2^*	0.30		
$\sigma_{2p_x}^*(\text{O}_2)$	0.06	$\sigma_{2p_x}^*(\text{O}_2)$	0.06	$\sigma_{2p_x}^*(\text{O}_2)$	0.06	$\sigma_{2p_x}^*(\text{O}_2)$	0.05		

^a $\sigma_{2p_x}(\text{O}_2)$ and $\sigma_{2p_x}^*(\text{O}_2)$ denote the bonding and antibonding orbitals, respectively, of the O–O moiety; $\pi_{2p_y}(\text{O}_2)$ denotes the analogue of the oxygen molecule π -bonding orbital of the O–O moiety, whose component 2p orbitals are perpendicular to the O–O bond and to the respective C–O–O plane (there is at least one such plane for each of the species considered); $\pi_{2p_x}(\text{O}_2)$ denotes the analogue of the oxygen molecule π -bonding orbital perpendicular to π_{2p_y} . For the description of the composite orbitals b₁, b₂, σ_1 – σ_4 , and σ_1^* – σ_4^* , see Scheme 4.

Scheme 4. Illustration of the Composite Orbitals of the Stationary Points in Oxygen Addition to butadiene and Benzene Referred to in Tables 3 and 6

The results obtained in this study also indicate that the cheletropic mechanism (mechanism B in Scheme 2) is unlikely. First, the putative transition structure SP'_{C_s} (Figure 1j), leading to the five-membered-ring intermediate I₂ (Figure 1c), is a second-order saddle point and has a relatively high energy (Table 1). The only route to I₂ goes through the linear intermediate I₁ and involves a transition structure T₃ relatively high in energy (Figure 1g, Table 1). The rearrangement of I₂ to P involves a transition structure T₄ (Figure 1h), which has the highest energy among all stationary points considered (Table 1); this energy is about 4 times higher than that of the direct rearrangement of I₁ to P. As shown (Table 1), I₂ itself has a higher energy, compared to that of the linear intermediate I₁, as estimated at the MCQDPT2/BSSE level, although the MCSCF energy alone is lower than that of I₁ (Table 1).

According to our calculations, the major barrier of oxygen addition to butadiene comes from the T₁ transition structure. The activation energies of oxygen addition to cyclic dienes in

**Figure 2.** First (a) and the second (b) mode with imaginary frequency of the second-order saddle point SP'_{C_s} in oxygen addition to butadiene. The frequencies are 660.7*i* and 137.4*i* cm⁻¹, respectively.

vacuo determined by Ashford and Ogryzlo³⁸ range from 3.9 kcal/mol for cyclopentadiene to 5.5 kcal/mol for 1,3-cyclohexadiene. These values are in fair agreement with the energy of the T₁ transition structure calculated in this study, which is 4.7 kcal/mol at the MCQDPT2 level (Table 1) and 9.9 kcal/mol after the BSSE correction. It should be noted that the BSSE correction at the MCSCF/PT2 or MCSCF/MCQDPT2 level is usually exaggerated. The uncorrected and BSSE-corrected values of the T₁ energy can therefore be considered the lower and upper limits, respectively, of the energy of T₁.

Finally, it should be noted that dienes usually occur in the *s-trans* conformation, and it is therefore reasonable to assume that this is the dominant conformation of the diene moiety attacked by oxygen to form the biradical intermediate I₁. In this case, the *s-trans* conformation of the diene moiety will be conserved in I₁ right after oxygen binding, and the formation of a cyclic product could occur only after I₁ reaches the *s-cis* conformation (upon a 180° rotation about the central C–C bond). As follows from Figure 1b, this bond is shorter than a

(38) Ashford, R. D.; Ogryzlo, E. A. *Can. J. Chem.* **1974**, *52*, 3544–3548.

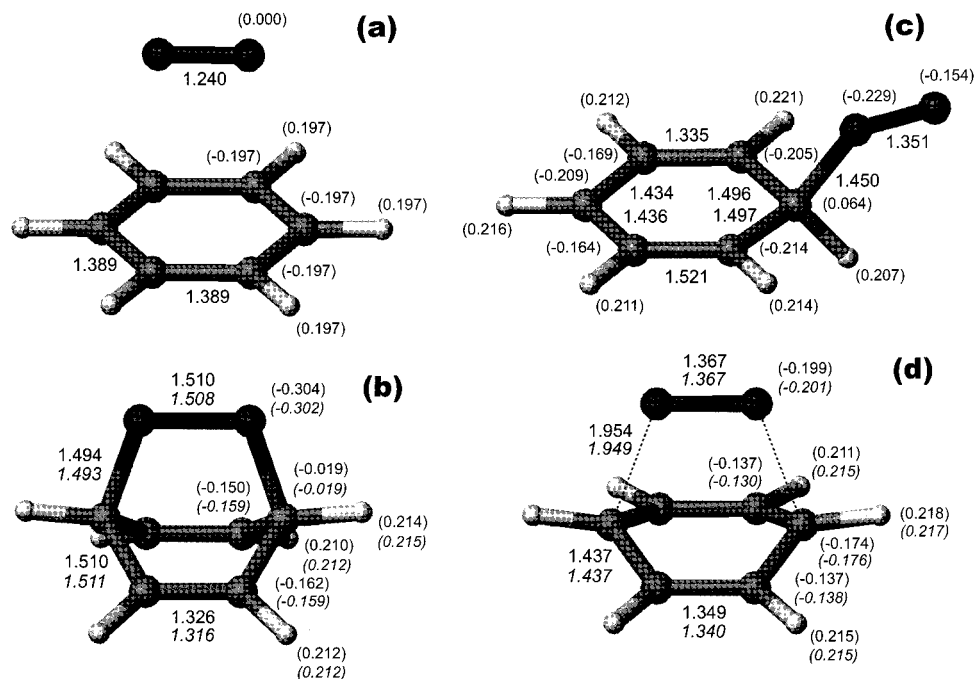


Figure 3. Stationary points on the benzene–singlet oxygen energy surface: (a) the reactants (S), (b) the product (P), (c) the linear intermediate (I_1), and (d) the *supra*–*supra* transition structure from S to P (SP_{C_s}). The lengths of selected bonds and selected interatomic distances in transition structures and Mulliken population charges are shown. The values in italics in parts (b) and (d) pertain to the (12,10) active space; the values for I_1 (part d) were calculated with the (10,8) active space only. The drawings were generated using MOLMOL.⁴⁰

Table 4. Relative Energies (with Respect to the Separated Reactants; kcal/mol) of the Stationary Points in Oxygen 1,4-Addition to Benzene

species		ΔE_{MCSCF}^a	$\Delta E_{MCSCF/BSSE}^a$	ΔE_{MCQDP2}^a	$\Delta E_{MCQDPT2/BSSE}^a$
transition structure	$T_{C_{2v}}$	40.86	43.09	21.15	29.27
		<i>41.67</i>	<i>43.98</i>	<i>17.12</i>	<i>25.25</i>
diradical intermediate	I_1	<i>36.49</i>	<i>36.75</i>	<i>18.71</i>	<i>26.69</i>
bicyclic product	P	16.45	19.52	3.66	17.11
		<i>18.82</i>	<i>21.95</i>	<i>1.76</i>	<i>11.82</i>

^a Values in italics pertain to the (10,8) active space.

single C–C bond and should therefore have a partially double character, which could result in a significant barrier to the corresponding internal rotation. We estimated this barrier by performing three constrained optimizations at the CAS MCSCF level of I_1 , with the values of the rotation angle constrained to 180°,³⁹ –90°, and 90°, respectively. The resulting energy barrier to internal rotation was 10.52 and 6.23 kcal/mol after the MCQDPT2 correction. These values are relatively low and can easily be overcome by thermal movement. Moreover, they are comparable with the energy differences between the second transition state T_2 and the intermediate I_1 obtained at the corresponding level of theory. Therefore, the mechanism of oxygen addition to dienes inferred from our study seems to be probable, even if the diene moiety is assumed to be in an *s-trans* conformation.

Oxygen 1,4-Cycloaddition to Benzene. The reaction routes studied are outlined in Figure 3b. The product formed, 2,3-dioxabicyclo[2.2.2]octa-5,7-diene, has C_{2v} symmetry with the peroxide moiety in the *syn* configuration (Figure 3b), consistent with the crystal structures of 1,4-peroxides formed from aromatic compounds.^{6,39} As opposed to the case of 1,3-butadiene, the

reaction is remarkably endoenergetic (Table 4); this can be attributed to (i) greater strains in the bicyclic compound formed on the addition, compared to a unstrained monocyclic compound formed from butadiene and oxygen, (ii) loss of aromaticity, and (iii) forcing the peroxide group into the *syn* configuration because of ring-closure constraints. The *supra*–*supra* oxygen approach that preserves the C_{2v} symmetry of the system passes through the first-order saddle point $T_{C_{2v}}$ (Figure 3d). There also exists a linear intermediate I_1 (Figure 3c), as in the case of oxygen addition to butadiene; however, we were unable to find a transition structure from the reactants to it. Every attempt to optimize the putative transition structure T_1 led to $T_{C_{2v}}$. It can therefore be concluded that I_1 can be formed only from P by breaking of one of the C–O bonds. This suggests that oxygen addition to benzene (and possibly to other aromatic compounds) occurs in one step. The absence of the second normal mode with imaginary frequency can be attributed to the *syn* configuration of the peroxide moiety in the product of this reaction, as opposed to the reaction of butadiene with oxygen, in which the species with *syn* configuration of the peroxide moiety is only a saddle point. It should also be noted that the estimated energy barrier to this process is much higher compared to 1,3-butadiene (Tables 1 and 5), and that $T_{C_{2v}}$ has an even higher relative energy compared to that of the second-order C_s saddle point in the case of butadiene; this can be attributed to strains in the bicyclic species formed and to the loss of aromaticity on oxygen addition. This difference is consistent with the fact that

(39) (a) Klein, C. L.; Stevens, E. D.; Zacharias, D. E.; Glusker, J. P. *Carcinogenesis* **1987**, *8*, 5–18. (b) Izuoka, A.; Murase, T.; Tsukada, M.; Ito, Y.; Sugawara, T.; Uchida, A.; Sato, N.; Inokuchi, K. *Tetrahedron Lett.* **1987**, *38*, 245–248. (c) Sawada, T.; Mimura, K.; Thiemann, T.; Yamato, T.; Tashiro, M.; Mataka, S. *J. Chem. Soc., Perkin Trans. 1* **1998**, 1369–1371.

(40) Koradi, R.; Billeter, M.; Wüthrich, K. *J. Mol. Graphics* **1996**, *14*, 51–55.

Table 5. Dominant Configuration State Functions^a of All Stationary Structures in Oxygen 1,4-Addition to Benzene

structure		CSF							coeff.	
transition state	$T_{C_{2v}}$	2	2	2	2	2	0	0	0	0.9381
		2	2	2	0	2	0	2	0	-0.1461
		2	2	2	1	1	1	1	0	0.1392
		2	0	2	2	2	2	0	0	-0.1215
		2	2	2	2	0	0	2	0	-0.1124
diradical intermediate	I_1	2	1	2	1	2	1	1	0	0.1079
		2	2	2	2	2	0	0	0	0.6958
		2	2	2	2	0	2	0	0	-0.6356
		2	2	2	2	1	1	0	0	0.1766
		1	1	2	2	2	1	0	1	0.1038
bicyclic product	P	2	2	2	2	2	0	0	0	0.9623
		2	0	2	2	2	0	0	2	-0.1820

^a The CSFs with coefficients greater than 0.1 in absolute value. See Table 6 for the order and description of orbitals.

Table 6. Character and Occupation Numbers of the MCSCF Natural Orbitals of All Stationary Structures in Oxygen 1,4-Addition to Benzene (See Table 3 for Explanation of Symbols)

	$T_{C_{2v}}$		I_1		P
$\sigma_{2s}(O_2)$	1.99	$\pi_{2p_y}(O_2)$	1.98	$\sigma_{2s}(O_2)$	2.00
$\sigma_{2p_x}(O_2)$	1.94	$\sigma_{2p_x}(O_2)$	1.94	$\sigma_{2p_x}(O_2)$	1.92
$\pi_{2p_y}(O_2)$	1.99	$\sigma_{2s}^*(O_2)$	2.00	$\sigma_{2s}^*(O_2)$	2.00
$\pi_{2p_z}(O_2)$	1.90	$\sigma(CO)$	1.97	σ_3	1.97
σ_4	1.92	b_1	1.07	σ_4	1.97
σ_3^*	0.06	b_2	0.95	σ_3^*	0.03
σ_4^*	0.13	$\sigma^*(CO)$	0.03	σ_4^*	0.04
$\sigma_{2p_x}^*(O_2)$	0.06	$\sigma_{2p_x}^*(O_2)$	0.06	$\sigma_{2p_x}^*(O_2)$	0.08

the rate constants of oxygen addition to naphthalene and anthracene derivatives are 1 or more orders of magnitude lower than in the case of acyclic dienes.³

As noted in the Methods section, to estimate the energies of the transition structure $T_{C_{2v}}$ and of the product P we extended the active space to (12,10), to avoid the possible bias connected with imbalanced active space of the isolated benzene molecule. (To save computational time, we did not perform such extended calculations for I_1 , which does not seem to occur on the reaction path of oxygen addition to benzene). The data in Table 4 indicate that the relative energies do not change significantly after extension of the active space; they appear to be shifted by a constant factor. The geometries of $T_{C_{2v}}$ and P also remain similar after extension of the active space (Figure 3). As in the case of butadiene, the additional two orbitals introduced have effectively 2 and 0 occupancy, respectively, in all species.

The stationary points $T_{C_{2v}}$ and I_1 have qualitatively the same electronic configurations, and their frontier orbitals have a form similar to those of the stationary points SP_{C_s} and I_1 of the reaction path of butadiene addition of oxygen (Tables 5 and 6). As in the case of butadiene, direct overlap between one of two degenerate HOMO orbitals of benzene and the $\pi_{2p_z}^*$ orbital of oxygen can develop, owing to their consistent phases, which allows for a one-step reaction with a symmetric transition structure $T_{C_{2v}}$. Because of formal transfer of one electron from benzene to oxygen, the transition structure is more polar than in the case of the linear transition structure T_1 corresponding to oxygen addition to butadiene (Figure 3d); this is consistent with the observed solvent effect on the rate constants of oxygen addition to aromatic compounds.³

Conclusions

The results of our study suggest that 1,4-oxygen addition to acyclic 1,3-dienes and to the aromatic compounds occurs through two different mechanisms: (i) a stepwise mechanism involving a linear biradicaloid intermediate (mechanism D of Scheme 2), as in the case of oxygen addition to isolated C=C bonds, and (ii) a single-step mechanism with a symmetric transition structure with significant charge transfer from the organic donor to oxygen (mechanism F and possibly G of Scheme 2, mechanism G taking place if the aromatic compound is not symmetric). This is consistent with the observed difference in the solvent effect on both processes,³ as well as with the observed nonstereospecificity of oxygen addition to some acyclic dienes.²⁵ The phase consistency of the frontier orbitals of the organic compound and oxygen allows for the second mechanism in both cases (as opposed to oxygen addition to isolated double bonds^{13,17,19}). However, in the case of oxygen addition to acyclic 1,3-dienes, it would lead in the first step to a species with the peroxide moiety in a syn configuration, which is a saddle point on the energy surface of the six-membered ring of the formed monocyclic peroxide. Conversely, the peroxide moiety in the bicyclic 1,4-peroxides formed from aromatic compounds is in the syn configuration owing to ring-closure constraints, and therefore the reaction can occur in one step with a symmetric transition structure. The syn configuration also occurs in 1,4-peroxides formed from cyclic 1,3-dienes, and it can therefore be supposed that the reaction occurs in one step also in this case.

On the basis of the results of earlier work^{17,19,20} and this study, it can be concluded that mechanisms involving cyclic zwitterionic intermediates peroxides (route C of Scheme 2) and 2,5-dihydrofuran 1-oxide derivatives (route B of Scheme 2) can be excluded, because the barriers to rearrangement of such intermediates to the final product are prohibitively high and each of them can be formed only from a linear biradicaloid intermediate. On the other hand, the calculated energy of 2,5-dihydrofuran 1-oxide (Table 1) is low enough that such species may be considered as probable intermediates in related reactions, such as the formation of hydroperoxides from phenols or naphthols through a proton transfer.

Acknowledgment. This work was supported by Grant PB 026/T09/97/12 from the Polish State Committee for Scientific Research. Calculations were carried out with the use of the resources and software at the Interdisciplinary Center for Mathematical and Computer Modeling (ICM), Warsaw, Poland, the Informatics Center of the Metropolitan Academic Network (IC MAN) at the Technical University of Gdańsk, and the IBM RS/6000 workstation at the Institute of Physics of Nicholas Copernicus University.

Supporting Information Available: Tables containing the Cartesian coordinates of the structures corresponding to the reaction of oxygen with benzene and with butadiene (PDF). This material is available free of charge via the Internet at <http://pubs.acs.org>.

JA001185C